Centrum voor Wiskunde en Informatica
REPORT*RAPPORT*

An adaptive image reconstruction method

M. Haindl

Computer Science/Department of Interactive Systems

CS-R9537 1995

Report CS-R9537
ISSN 0169-118X

CWI
P.O. Box 94079
1090 GB Amsterdam
The Netherlands

An Adaptive Image Reconstruction Method

Michal Haindl
CWI
P.O. Box 94079, 1090 GB Amsterdam, The Netherlands

email mh@cwi.nl

Abstract

A new adaptive regression type of image destriping method is introduced to reconstruct missing lines in multispectral images. The method uses available information from the failed pixel surrounding due to spectral and spatial correlation of multispectral data. The reconstruction is based on two mutually competing adaptive regression models from which the locally optimal predictor is selected.

AMS Subject Classification (1991): 62M30, 68U10
CR Subject Classification (1991): I.4.5
Keywords & Phrases: Image reconstruction, adaptive modelling.
Note: This paper was presented on the 12th IAPR Int. Conf. on Pattern Recognition in Jerusalem, 1994.

1. Introduction

Using scanners or CCD cameras for image data acquisition often involves removing errors caused if one of the detectors fails to function, or goes out of adjustment, during a scan. If the scanner is on board of a satellite, there are very often data losses during the transmission to Earth. Another source of errors can be an interference with some disturbing data source like an aircraft interception radar in radio-spectrograph observations, etc. This error is often called a line dropout or a line striping. Methods used to reconstruct missing multispectral data are mostly very simple and do not use all attainable information due to large correlation between single image elements.

There are several ways of how to reconstruct failed image data. NASA ground processing replaces the failed detector scan line with the scan line of the detector immediately above it (we will refer to this method further as A). This scheme can cause [1] very observable distortions in the final image products, especially images of high contrast cultural features. It has been suggested a variant of mentioned method to linearly interpolate between the line above and line below the failed detector line - method B, or from six neighbouring pixels - method C. This doesn't solve the problem. Even interpolation with higher order curves, such as quadratic fit, are of no help [1]. Three more sophisticated template-like methods were suggested in [1] : Template Replacement (D), Template Replacement with Error Adjustment (E) and Quadratic Vertical Fit with Template Data (F). The Template Replacement method directly substitutes a failed detector line with detector line from similar (well correlated) band, after scaling its output intensity so that its range is similar to the other lines of the failed line spectral band. The coefficients of the quadratic are determined by a least squares fit to the actual data in a five pixel vertical slice centered around each failed detector pixel. The data value used for the failed (centre) pixel in the slice is calculated as in (D) algorithm. Test results in [1] show in low contrast regions slightly off colour stripe after applications of algorithms (D) and (E). The problem of algorithm (F) is that it produces a lower contrast value than would be expected in light contrast areas. Finally we have proposed the regression method (G) in [3], which clearly outperforms these above mentioned reconstruction methods.

In this paper we present an improvement of our reconstruction method, stemmed from the obser-

vation that the method performance can further improve if its necessary data approximation is made from locally optimal data site. The presented method (H) selects a locally optimal predictor from two competing symmetrical adaptive predictors for each pixel to be reconstructed.

This paper is organised as follows. In Section 2, a proposed method general concept under a Bayesian framework is introduced. Section 3 completes the algorithm with a locally optimal model selection rule design. Section 4 deals with numerical realisation problems while Section 5 contains the experimental results in the processing of radio-spectrograph observations of the solar radio emissions and remotely sensing imagery data.

2. The Monospectral Line Regression Model

We assume the monospectral line to be modelled:

$$Y_{\acute{t}} = \sum_{i \in I_{\acute{t}}} a_i Y_{\acute{t}-i} + E_{\acute{t}} \tag{1}$$

with a multiindex $\acute{t} = (m, n, d)$, and where $Y_{\acute{t}}$ is a reconstructed monospectral pixel value, m is a row indicator, n a column indicator , $d(d \geq 1)$ denotes the number of spectral bands and also a spectral band with line to be reconstructed (an arrangement of spectral bands is our choice) , a_i are unknown model parameters, $E_{\acute{t}}$ is the white noise component. $I_{\acute{t}}$ is some neighbour index shift set excluding unknown data $(0, j, 0) \notin I_{\acute{t}}$ only.

Let us denote another multiindex $t = (m, n, d)$ and choose a direction of movement on the image plane to track failed line $t-1 = (m, n-1, d), t-2 = (m, n-2, d), \ldots$ E_t is the white noise component with zero mean and constant but unknown dispersion Ω. We assume that the probability density of E_t has a normal distribution independent of previous data and is the same for every time t. Let us formally assume knowledge of missing data, then the task consists of finding the prediction density given the known process history:

$$Y^{(t-1)} = \{Y_{t-1}, Y_{t-2}, \ldots, Y_1, Z_t, Z_{t-1}, \ldots, Z_1\} \ , \tag{2}$$

where Z is defined in (7). On this density we have chosen the conditional mean estimator for data reconstruction, because of its optimal properties :

$$\tilde{Y}_t = E[Y_t | Y^{(t-1)}] \ . \tag{3}$$

Let us rewrite the regressive model (1) into the matrix form:

$$Y_t = P^T Z_t + E_t \ , \tag{4}$$

where

$$P^T = [a_1, \ldots, a_\beta] \tag{5}$$

is the $1 \times \beta$ unknown parameter vector,

$$\beta = card I_{\acute{t}} \ , \tag{6}$$

and we denote the $\beta \times 1$ vector

$$Z_t = [Y_{t-i} : \forall i \in I_{\acute{t}}]^T \ . \tag{7}$$

Assuming normality of the white noise component E_t, conditional independence between pixels and the prior probability density for the unknown model parameters chosen in the form

$$p(P,\Omega^{-1}|Y^{(0)}) = (2\pi)^{-\frac{\gamma(0)}{2}}\ |\Omega|^{-\frac{\gamma(0)}{2}} \exp\left\{-\frac{1}{2}tr\{\Omega^{-1}\begin{pmatrix}-I\\P\end{pmatrix}^T \Psi_0 \begin{pmatrix}-I\\P\end{pmatrix}\}\right\} \tag{8}$$

where Ψ_0 is a positive definite $(\beta+1)*(\beta+1)$ matrix and

$$\gamma(0) > d\ . \tag{9}$$

We have derived [3] the conditional mean value to be:

$$\tilde{Y}_t = \hat{P}_{t-1}^T Z_t\ . \tag{10}$$

Where the following notation is used:

$$\hat{P}_{t-1} = \Psi_{z(t-1)}^{-1}\Psi_{zy(t-1)}\ , \tag{11}$$

$$\Psi_{t-1} = \tilde{\Psi}_{t-1} + \Psi_0\ , \tag{12}$$

$$\tilde{\Psi}_{t-1} = \begin{pmatrix}\tilde{\Psi}_{y(t-1)} & \tilde{\Psi}_{zy(t-1)}^T\\ \tilde{\Psi}_{zy(t-1)} & \tilde{\Psi}_{z(t-1)}\end{pmatrix}\ , \tag{13}$$

$$\tilde{\Psi}_{y(t-1)} = \sum_{k=1}^{t-1} Y_k Y_k^T\ , \tag{14}$$

$$\tilde{\Psi}_{zy(t-1)} = \sum_{k=1}^{t-1} Z_k Y_k^T\ , \tag{15}$$

$$\tilde{\Psi}_{z(t-1)} = \sum_{k=1}^{t-1} Z_k Z_k^T\ . \tag{16}$$

Later two additional notations will be useful:

$$\gamma(t-1) = \gamma(0) + t - 1\ , \tag{17}$$

$$\lambda_{t-1} = \Psi_{y(t-1)} - \Psi_{zy(t-1)}^T \Psi_{z(t-1)}^{-1}\Psi_{zy(t-1)}\ . \tag{18}$$

It is easy to check [3] also the validity of recursive equations (19)-(21). We assume slowly changing parameters, so these equations were modified with a constant exponential forgetting factor (α) to allow parameter adaptation. This factor was used in our experiments with a standard value $\alpha = 0.99$.

$$|\Psi_{z(t)}| = |\Psi_{z(t-1)}|\alpha^{2\beta}(1 + Z_t^T\Psi_{z(t-1)}^{-1}Z_t) \tag{19}$$

$$\lambda_t = \lambda_{t-1}(1 + (Y_t - \hat{P}_{t-1}^T Z_t)^T \lambda_{t-1}^{-1}(Y_t - \hat{P}_{t-1}^T Z_t)(\alpha^2 + Z_t^T\Psi_{z(t-1)}^{-1}Z_t)^{-1}) \tag{20}$$

$$\hat{P}_t = \hat{P}_{t-1} + (\alpha^2 + Z_t^T\Psi_{z(t-1)}^{-1}Z_t)^{-1}\Psi_{z(t-1)}^{-1}Z_t(Y_t - \hat{P}_{t-1}^T Z_t)^T \tag{21}$$

To evaluate predictor (10) we need to compute the parameter estimator (11) or (21), but we do not know necessary past data Y_t. This problem is solved using the approximation based on spatial correlation between close lines

$$\tilde{Y}_t \doteq \tilde{P}_{t-1}^T Z_t \ , \tag{22}$$

where $\tilde{P}_{t-1}$ is corresponding parameter estimator (11),(21) for the nearest known line with known contextual neighbors (7) to our reconstructed one in the spectral band d . Note different Z (7) in (22) and (15),(16),(19)-(21).

3. Locally Optimal Model Selection

Let us assume two regression models (4) M_1 and M_2 with the same number of unknown parameters ($\beta_1 = \beta_2 = \beta$) and mutually symmetrical neighbour index shift sets $I_{1,t}, I_{2,t}$ with the missing line being their symmetry axis. Now the presented algorithm can be completed in the form (23)

$$\tilde{Y}_t \doteq \begin{cases} \tilde{P}_{1,t-1}^T Z_{1,t} & \text{if} \quad p(M_1|Y^{(t-1)}) > p(M_2|Y^{(t-1)}) \\ \tilde{P}_{2,t-1}^T Z_{2,t} & \text{otherwise} \end{cases} \tag{23}$$

where $Z_{i,t}$ are data vectors corresponding to $I_{i,t}$. Following the Bayesian framework accepted in our paper and choosing uniform model priors (having no contrary information) $p(M_i|Y^{(t-1)}) \sim p(Y^{(t-1)}|M_i)$ the simultaneous conditional probability density can be evaluated from

$$p(Y^{(t-1)}|M_i) = \int\int p(Y^{(t-1)}|P,\Omega^{-1}) p(P,\Omega^{-1}|M_i) dP d\Omega^{-1} \ . \tag{24}$$

Under already assumed conditional pixel independence, the analytical solution has form

$$p(M_i|Y^{(t-1)}) = k \ |\Psi_{i,z(t-1)}|^{-\frac{1}{2}} \ \lambda_{i,t-1}^{-\frac{\gamma(t-1)-\beta+2}{2}} \tag{25}$$

where k is a common constant. To evaluate $p(M_i|Y^{(t-1)})$, we have to use similar approximation (22) as for the predictor (10). All statistics related to a model M_1 ((15),(16),(21),(25)) are computed from data on one side of the reconstructed line while symmetrical statistics of the model M_2 are computed from the opposite side.

In the case when some data necessary for the approximation are missing the corresponding model probability is set to zero

$$p(M_i|Y^{(t-1)}) = 0 \ . \tag{26}$$

If the reconstructed line is located in a boundary image area then reconstruction algorithm uses only one model (one of model probabilities is permanently zero).

4. Numerical Realization

The predictors in (23) can be evaluated using updating of matrices $\Psi_{i,t}$ (12) and their following inversion. Another possibility is direct updating of $\hat{P}_{i,t}$ (21). To ensure the numerical stability of the solution , it is advantageous to calculate (21) by the means of the square-root filter , which guarantees the positive definiteness of matrix (12). The filter updates directly the Cholesky square root of matrices $\Psi_{i,t}^{-1}$. Alternatively it is possible to use the UDU filter for this purpose. Initialisation of recursive equations (19)-(21) must keep the condition of positive definiteness of matrices $\Psi_{i,0}$ (8). We implemented in our algorithm the uniform priors start :

$$\Psi_{i,0} = I \ . \tag{27}$$

This solution not only conforms with initial lack of information at the start of algorithm, but also simplifies solution of the integral (24). Another possibility could be for example a local condition start, which ensures quicker adaptation . However, in an unrepresentative start window the predictor adaptation is delayed.

5. Experimental Results

In this section we present simulation results of the proposed reconstruction method and compare them with methods briefly surveyed in the introductory section. The performance of methods is compared on artificially created failed lines (removed from the unspoiled parts of images so the original data are known) using the criterion of mean absolute difference between original and replaced pixel values

$$MAD = \frac{1}{n} \sum_{i=1}^{n} |Y_i - \tilde{Y}_i| \ .$$

Pixels corresponding to the $I_{i,t}$ are denoted $*$ and the reconstructed pixel $\circ$, respectively.

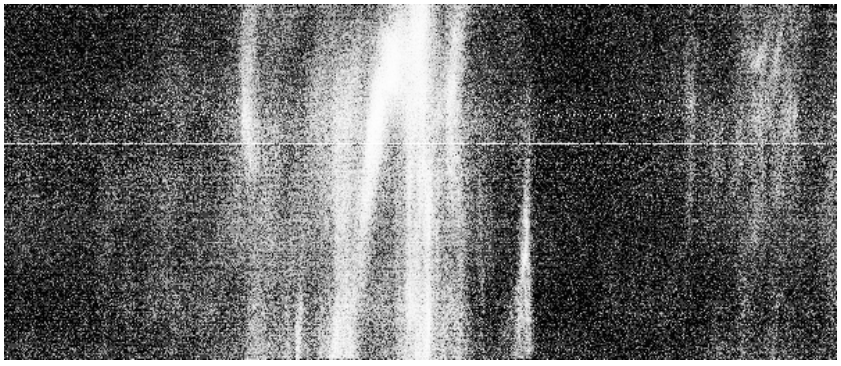

The first example is the defect radio-spectrograph image shown in Fig.1 from the Ondřejov Observatory 1000 - 2000 MHz radio-spectrograph observation of the solar radio emission. The fully automatic spectrograph [4] has the time resolution 0.1 s (10 sweeps per second) the frequency band is divided into 256 channels (the frequency resolution of about 4 MHz) and the grey level range of pixels is 0-2800. Observations with this new radio-spectrograph as a part of a complex device of the 100 - 4200 MHz radio-spectrograph contribute to elucidate the role of past drift burst in the solar flare process and to obtain an additional radio information to the results of the YOHKOH mission. Unfortunately these radio data are often damaged with an interference of the aircraft interception radars (military or civil). Considering the fact of secrecy of the interfering radar channel it is not possible to avoid these defects during solar observation. The optimal reconstruction models M_i for the radio-spectrograph were found to be:

$$M_1 = \begin{array}{ccccc} & * & & * & * \\ * & * & \circ & * & * \\ & * & & * & * \end{array} \qquad M_2 = \begin{array}{ccccc} & * & * & & * \\ * & * & * & \circ & * & * \\ & * & * & & * \end{array}$$

The second tested image was the agricultural type of the Thematic Mapper seven spectral band subscene from North Moravia. The failed line was located in the TM1 band. and selected models are:

$$M_1 = \begin{array}{ccccc} & & * & & * \\ & * & * & \circ & * \\ & & * & & * \end{array} \qquad M_2 = \begin{array}{ccccc} & & * & & * \\ & * & \circ & * & * \\ & & * & & * \end{array}$$

The last two examples are SPOT multispectral image (agricultural scene from Moravia, failed line located in the green visible band)

$$M_1 \quad \begin{matrix} * & & & & \\ & * & \circ & * & * \end{matrix} \qquad M_2 \quad \begin{matrix} & & & & * \\ * & * & \circ & * & \end{matrix}$$

and SPOT panchromatic image (agricultural scene from vicinity of La Rochelle, both models are $\begin{matrix} * & * & \circ & * & * \end{matrix}$).

monospectral			multispectral	
method	radar MAD	SPOT MAD	TM MAD	SPOT MAD
A	701	2.8	24	1.25
B	412	1.3	20	0.7
C	394	1.8	19	0.9
D	-	-	23	2.6
E	-	-	21	1.1
F	-	-	19	1.5
G M_1	400	1.2	17	0.65
G M_2	135	1.23	16	0.7
H	135	1.1	15	0.6
H	134	0.74	10.7	0.35

Result table shows superiority of our method over the classical ones with the last row demonstrating isolate pixels reconstruction (no approximation needed). The radar example demonstrates properly found better estimation data side in the case of one superior side, on the remaining examples the optimal side is oscillating so single model method (G) cannot reach performance of method H even if repeated on both corresponding sides.

6. Conclusion

The results of our testing are encouraging. The proposed method was always the best one in all our experiments. The supremacy of the method is higher with an increasing number of correlated spectral bands but even on monospectral images (the radio-spectrograph and SPOT panchromatic examples) is also the best one. We have never seen any other scheme typical image defects (off colour stripe, colour gaps, horseshoe effect) applying the regression method. The advantage of the presented method over our single model regression method G [3] lies in automatic selection of the optimal side (more correlated data) for line reconstruction. If the optimal side is the same for all reconstructed pixels then similar effect can be reached running the method G twice on corresponding data sides and selecting the reconstruction model which has higher probability. But very often this optimal side is changing and therefore is not possible (see the last three examples) to approach quality of the presented method with the method G.

Our method can also be used if more than one of the monospectral line components are missing. In such a case we can apply our method repeatedly (model is modified to exclude missing data) to all missing monospectral lines. In the case of all spectral line components missing we can easily generalize model to a multidimensional regression model and follow the same reconstruction strategy.

Finally if the method is used for isolated image pixels reconstruction then the predictor and similarly the model probability expression do not need any data approximation and the regression method performs better then for line reconstruction and much better then any of classical methods.

References

1. Bernstein, R. - Lotspiech, J.B. - Myers, H.J. - Kolsky, H.G. - Lees, R.D. *Analysis and Processing of Landsat-4 Sensor Data Using Advanced Image Processing Techniques and Technologies.* IEEE Trans on Geosci., vol **GE-22** , no.3, 1984, 192-221
2. Broemeling,L.D. *Bayesian Analysis of Linear Models.* New York, Dekker 1985
3. Haindl,M.-Šimberová,S. *A Multispectral Image Line Reconstruction method.* In: Theory & Applications of Image Analysis. P. Johansen, S. Olsen Eds., World Scientific Publishing Co., Singapore, 1992.
4. Jiřička,K. - Karlický,M. - Kepka,O. - Tlamicha,A. *Fast Drift Observations with the New Ondřejov Radiospectrograph.* Solar Physics 147,Letters, 1993, 203-206.